Instrument Science Report WFC3 2009-45

WFC3 SMOV Programs 11424, 11434: UVIS Channel On-orbit Alignment

G. Hartig, L. Dressel, and T. Delker
14 December 2009

ABSTRACT

Following the insertion of WFC3 into the HST observatory during Servicing Mission 4, we aligned the UVIS and IR channels, independently, to the telescope early in the SMOV4 instrument verification campaign. Using a variety of techniques, and accounting for the OTA temporal focus variation, we adjusted the instrument corrector mechanisms to optimize image quality. The UVIS channel alignment observations, analysis techniques and resulting adjustments are described herein; alignment of the IR channel is treated in a separate report.

Introduction

Each of the HST science instruments (SIs) installed in the observatory on-orbit during servicing missions must be aligned to the telescope. Although WFC3 was shown to be well-aligned to its nominal optical telescope assembly (OTA) interface, as represented by the ground support test hardware during pre-launch testing (Hartig, 2008), the instrument latch position uncertainties and the effects of gravity release, in particular, are sufficiently large that the stringent requirements for pupil alignment and focus cannot be met with ground testing and adjustment alone. The image quality is particularly sensitive to registration of the OTA exit pupil with the SI entrance pupil, since the SI must correct the large spherical aberration produced by the OTA. Pupil shear of less than 1% results in noticeable coma. Hence the SIs generally incorporate corrector mechanisms to permit accurate pupil alignment as well as to adjust focus. (An exception is the Cosmic Origins Spectrograph, for which pupil alignment is achieved by repointing the observatory and repositioning its aperture.)

The corrector mechanisms used in both the UVIS and IR channels of the WFC3 are based on the design employed by the ACS, which consists of a nested eccentric cylinder pair ("Wally Wobbler") to effect tip and tilt of the mirror which serves to image the OTA pupil on the corrective optic, riding on a linear focus stage, all driven by redundantly-wound stepper motors. Resolvers provide absolute position feedback for the cylinders, while linear variable differential transducers (LVDTs) indicate the focus position; these positions are

downlinked in the engineering telemetry stream and included in the support (.spt) files produced by the OPUS pipeline. Because the optical beam is folded at the mirror on the corrector mechanism, linear motion of the focus stage also produces some pupil shear, which must be accounted for in optical performance analyses. This coupling is particularly severe for the IR channel, as discussed by Hartig (2005). With a perfect focus stage this effect would be predictable, but in practice the pupil shear produced by the UVIS stage was found to be non-repeatable, complicating the analysis.

Focus adjustment, while inherently straightforward, is complicated by the temporal variation of the OTA focus ("breathing") caused by thermally-induced changes in the telescope structure. While this effect has been modeled using data from the OTA thermal sensors, the model does not accurately predict the absolute focus over the long term, but can be effectively used to improve relative focus assessment through a single orbit. Final focus adjustment must therefore be based on the ensemble of focus measurements obtained through the alignment process.

This report details the on-orbit alignment process, describing the observations and analysis techniques used to rapidly converge on the near-optimal alignment of the UVIS channel. The IR channel alignment is similarly treated in a companion report (Hartig, et al. 2009). A chronology of the measurements and a log of the corrector mechanism adjustments are presented. Final confirmation of the imaging performance is described elsewhere (Hartig, 2009).

Observations

The alignment program proceeded in two stages, beginning with relatively coarse, five position focus sweeps in 500 step increments from -1000 to +1000 steps from the current nominal position. These produce image sets with sufficient focus diversity (± 1.65 mm at the detector, corresponding to 38 nm RMS focus or $\lambda/11$ at 410 nm) which permit reasonably accurate phase retrieval (PR) assessment of the wavefront error (WFE), especially coma, from which pupil alignment corrections can be determined. While greater focus range would yield greater WFE measurement accuracy, motion of the focus stage was limited due to thermal concerns (the motor temperature rises rapidly during actuation) and the desire not to move to positions too far from best focus, at which severe impact to the scientific capability of the instrument would result in the very unlikely event of stage failure.

These focus scans were implemented with SMOV4 program 11424, which specified three visits, separated by at least 48 hrs., to permit data acquisition, analysis and uplink of the required corrections before the next observation set was obtained. All of the observations are specified with relative focus and cylinder motor step offsets. Each visit may result in adjustments to the corrector mechanism inner or outer cylinder rotational positions, to improve pupil alignment, and/or focus stage position. The adjustments are effected by real-time commands of relative motor step offsets, specified in Operations Requests to the STOCC at GSFC and generally routed through the STScI SI commanding group. The UVIS detector was operated at its nominal temperature, –83C, and nominal gain (1.5 e^- /DN), and all images were obtained with the full field format, with CR-split pairs to permit cosmic ray rejection.

After the alignment was nearly optimized, a fine 9-position focus scan, using 250-step increments, was executed with program 11434, followed by a 9 point tip/tilt raster, with ±3 step offsets of each cylinder from its current position, to assure that the pupil alignment had been achieved. It is essential that the focus be set before making the final adjustment of the tip/tilt (pupil) alignment because of wobble in the linear focus stage, which produces significant, unpredictable pupil shear as focus is adjusted. While this effect was seen during ground testing, it was found to be considerably worse and less repeatable on-orbit. Because of an FGS guide star lock failure in the first (focus scan) visit, extra visits were scheduled to repeat the fine focus scan (visit 51) and following tip/tilt raster (visit 52).

The target for both programs is a field in NGC-188, an astrometric old open cluster, chosen to yield a reasonable density of appropriately bright stars to permit accurate encircled energy measurements while sampling the FOV well with relatively short exposures in the F410M filter. The moderate bandpass and central wavelength of this filter permit accurate PR analysis to determine the WFE. The high latitude of NGC-188 makes it available year-round, and, if guide stars are selected from the astrometric catalog (ID=ZZZZ), then absolute boresight measurements are also possible. The chosen field is centered on the star designated #58 in the astrometric catalog; this star turns out to be binary, so is not particularly useful in itself for either astrometric or imaging performance evaluations, but there are many stars in the field that do support both analyses.

Logs of the observations for all visits of both programs are listed in Appendix A. These include the absolute corrector mechanism positions for each exposure, indicated as triads of focus stage LVDT, and inner and outer cylinder resolver readbacks, in that order. The modeled OTA breathing (brth) is also listed, in microns of secondary mirror (SM) despace.

Analyses

The NGC-188 field images were analyzed by first identifying suitable stars, which are of sufficient signal level (>3-5 kDN in the peak px), and isolated from neighbors and field edges, bad pixels, etc. in order to permit accurate encircled energy computation. This selection was accomplished with IDL tool *findstars*, which, after automatically selecting suitable PSFs, permits manual inspection of the results, enabling further vetting. About 30 stars, distributed over the field, were typically selected this way for analysis. Figure 1 displays the field with selected stars identified from program11424 visit 3.

The focus scan measurements were made using idl tool *fscan_smov*, which computes the encircled energy (EE) in a 0.15 arcsec diameter for each of the selected stars at each focus position, excludes outliers, and plots the EE averaged over the field vs. focus. The OTA breathing model was used to estimate the telescope focus state at the time of each observation and correct the nominal focus positions. A parabola was then fit to the data to determine the optimal focus setting. Figure 2 shows the results of the program 11424 visit 3 scan. The error bars represent the standard deviation of the measurements over field for each focus setting.

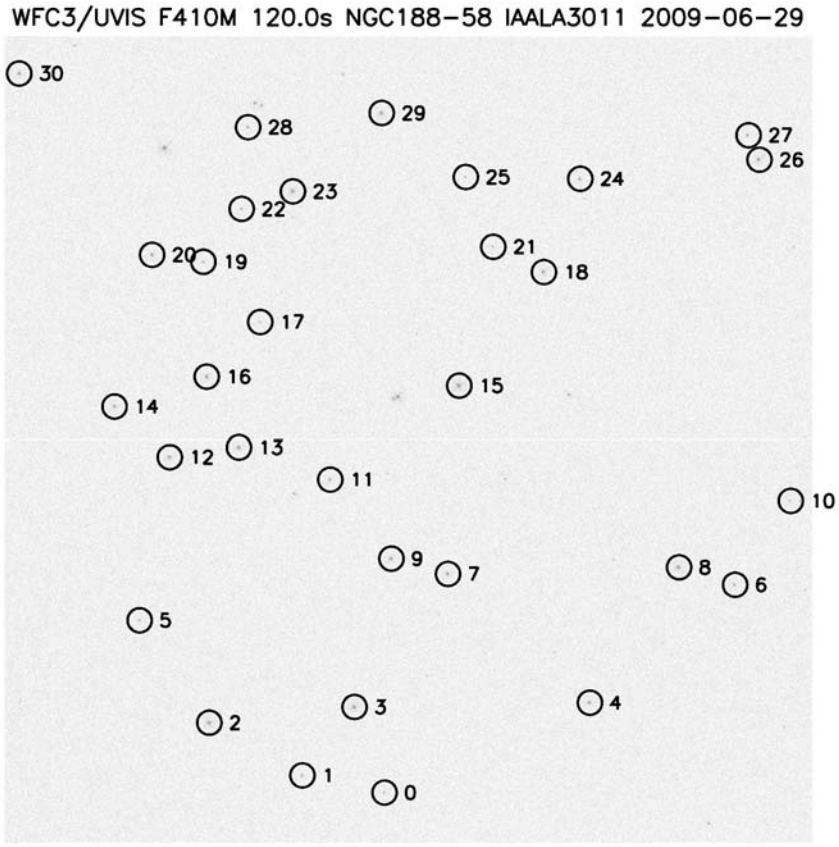

Figure 1. The NGC 188 field showing stars selected for analysis from visit 3 of program 11424.

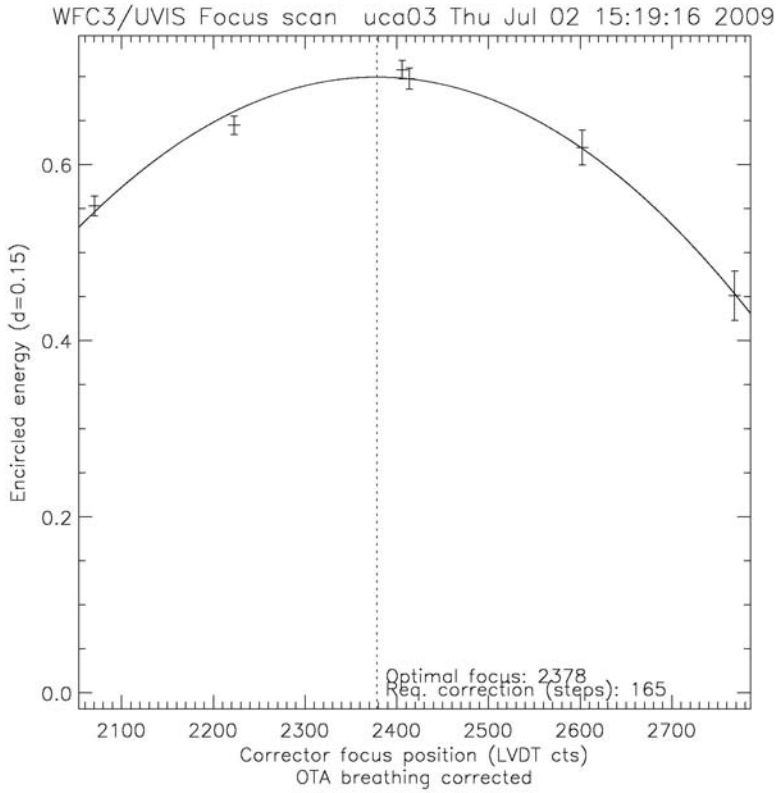

Figure 2. Encircled energy vs focus position for visit 3 of program 11424.

The pupil alignment is evaluated with IDL tool *align_smov*, which uses *wfc3fitc* to perform PR analysis to determine the low-order WFE for each star, simultaneously fitting images from the 5 focus positions. The WFE data are then used to compute the corrector cylinder offsets required to compensate the measured coma using sensitivity factors and coordinate transformations determined empirically or by modeling (and confirmed by measurement), as encoded in *wfc3_uvis_corr*. Figure 3 shows the resultant map of cylinder step corrections for each field point and the mean over all of the measured points, which was adopted as the desired offset to be applied. The scatter in the results represents the instrinsic field-dependent design residual and internal alignment errors as well as the measurement uncertainty, which varies from star to star depending on the signal level, presence of uncorrected detector artifacts and CRs, etc.

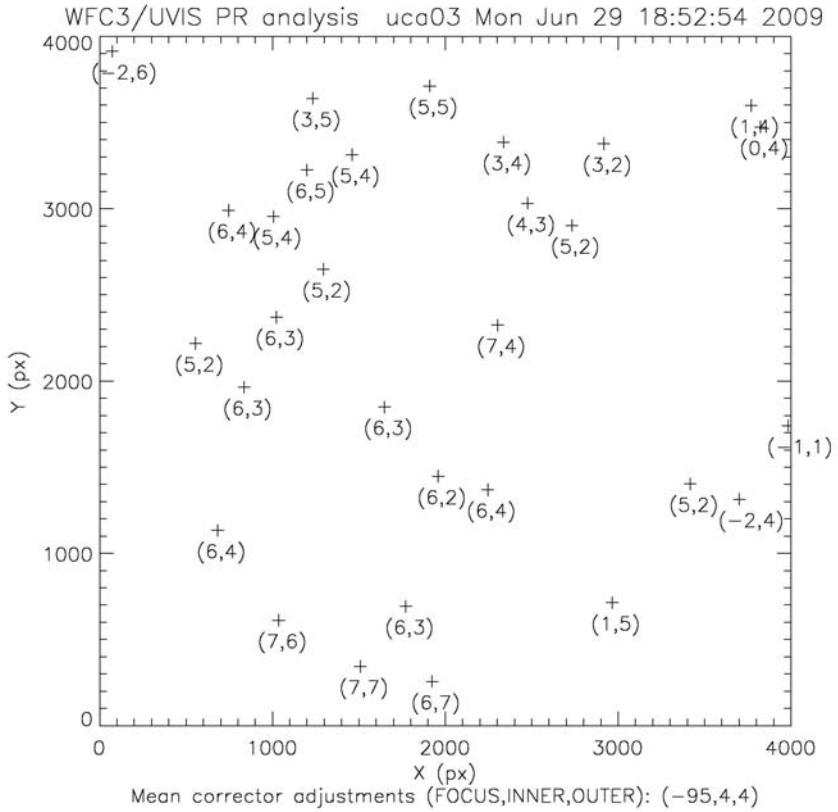

Figure 3. PR results for visit 3 of program 11424 showing the corrector cylinder offsets required to minimize coma at each field point.

As mentioned above, the use of the corrector focus stage to provide focus-diverse image sets for PR analysis results in unpredictable amounts of pupil shear (and resulting coma) due to wobble of the mirror on the stage. This was ameliorated by using the measured image location offsets to estimate the mechanism-induced coma contribution and add it to the WFE estimate at each focus position during the iterative fit process in *wfc3fitc*. The wobble also caused problems with CR rejection using the CR-split image pairs, since the images are not well-registered immediately following a focus move, probably due to a thermally-induced drift in the mechanism. As a result, special processing was required to identify and correct CRs in the vicinity of the star images and the images were then measured individually rather than after combining. In some cases the first image after a

focus move was clearly smeared as a result of the mechanism drift and was rejected from the analysis.

The program 11434 tip/tilt raster images were analyzed using both EE and PR techniques on each image. The resultant coma estimates were plotted against relative inner and outer cylinder step position, with contours fit to visualize the coma distribution. Because there is no focus diversity in these PR analyses (single images near optimal focus were fit), the accuracy is poor relative to that obtained with the focus scan data. The EE measurements were also plotted in the same manner. These results are depicted in Figure 4 for the final, visit 52, alignment observation, and indicate that near optimal alignment had been achieved, with only small cylinder offsets required. However, the results are ambiguous, since the coma is minimized near the (+3,-3) position, whereas the EE is maximized at (-3,-3). The results from visit 2 displayed similar offsets between the EE and PR results. We adopted the EE results as being more trustworthy and indicative of the true optical performance and requested a final adjustment of -3 steps on each cylinder.

The final, fine focus scan data were treated in the same fashion as the coarse scans described above. Because the OTA long term focus was determined to have drifted over the past several years to be sufficiently long of the common position optimal for the pre-SM4 instruments (ACS, STIS, NICMOS), an adjustment of the OTA SM despace by +3 μ was planned for 20 July 2009. The optimal adjustment was estimated at 2.5 μ and an additional 0.5 μ was added to overcompensate since continued focus drift is expected. The final WFC3 focus setting anticipated this OTA focus adjustment and included a +260 step offset to compensate the 2.5 μ SM shift in addition to the +100 step offset deduced from the ensemble of focus scans to date.

Table 1 lists each of the corrector adjustments made throughout the SMOV4 alignment program to achieve near-optimal optical performance. The net adjustments indicate that the instrument was originally positioned in the HST observatory within ~ 0.25 mm of optimal focus and ~ 3 arcminutes of the desired chief ray angle.

Table 1. WFC3/UVIS Corrector Adjustment Log

		Focus		Inner Cylinder		Outer Cylinder	
date	prop:visit	Δsteps	LVDT	Δsteps	resol	Δsteps	resol
24-Jun	First Light		2525		8459		53311
25-Jun	11424:1	-150	2478	-5	8155	-16	52399
27-Jun	11424:2	-450	2316	-4	7942	-6	52024
29-Jun	11424:3	0	2316	4	8047	4	52277
4-Jul	11434:2	0	2316	0	8047	-1	52276
6-Jul	11434:51	360	2437	0	8047	-3	52088
8-Jul	11434:52	0	2437	-3	7891	-3	51903
Net adjustment:		-240		-8		-25	

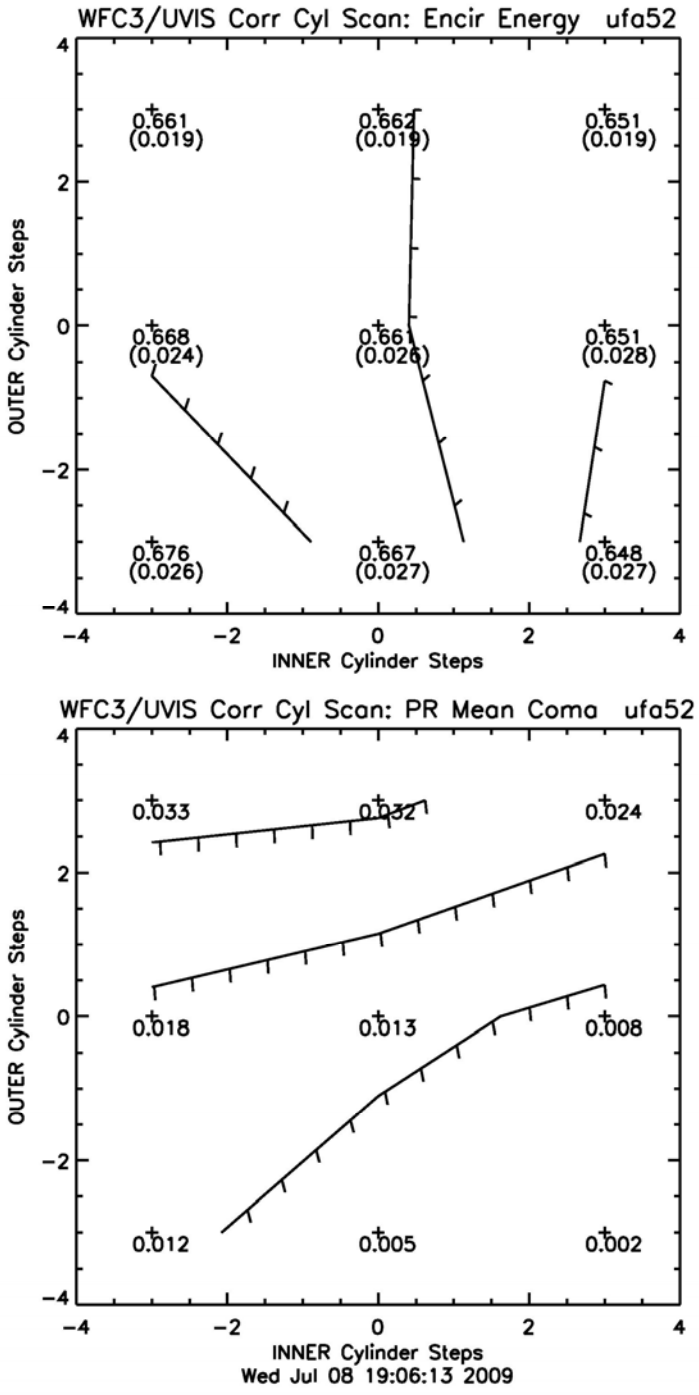

Figure 4. EE and PR results for the corrector cylinder raster scan of visit 52 of program 11434.

Conclusion

The WFC3 UVIS channel was successfully aligned on-orbit during the scheduled SMOV4 program. Although a guide star acquisition failure and unexpectedly large wobble of the corrector focus stage complicated the timeline and analysis, final alignment was achieved on 10 July 2009, with uplink of the last small adjustments. Because the focus, determined with only a few observations, is somewhat uncertain due to the OTA breathing, continued monitoring of the image quality at a larger variety of breathing states may indicate that further adjustment is warranted. If this is attempted, a cylinder scan should be scheduled after the focus adjustment to enable compensation for any pupil shear that may occur as a result of focus stage wobble.

Acknowledgements

The authors are grateful to Matt Lallo, Colin Cox and Chris Long for assistance in determining the OTA focus state and providing the breathing model data, which were essential to setting the WFC3 focus.

References

Hartig, G.F. “WFC3 IR Channel Corrector Alignment”, STScI ISR WFC3-2005-03, 2005

Hartig, G.F. “WFC3 Optical Alignment Characterization in Thermal-Vacuum Test #3”, STScI ISR WFC3-2008-32, 2008

Hartig, G.F. “WFC3 SMOV Proposals 11436/8: UVIS On-orbit PSF Evaluation”, STScI ISR WFC3-2009-38, 2009

Hartig, G., Dressel, L., and Delker, T. “WFC3 SMOV Proposals 11435/7: IR Channel On-orbit Alignment”, STScI ISR WFC3-2009-46, 2009

Appendix A. Observation Logs

11424\visit1

rootname	obs_date	obs_time	exptime	brth	corrector_pos
iaal01hxq	09-06-25	06:18:14	60.00	2.1	(2527,8459,53311)
iaal01hyq	09-06-25	06:21:26	60.00	1.7	(2527,8459,53311)
iaal01i4q	09-06-25	06:57:08	60.00	0.3	(2191,8459,53311)
iaal01i5q	09-06-25	07:00:20	60.00	0.6	(2191,8459,53311)
iaal01i8q	09-06-25	07:15:57	60.00	0.9	(2354,8459,53311)
iaal01i9q	09-06-25	07:19:09	60.00	0.9	(2354,8459,53311)
iaal01j1q	09-06-25	08:33:07	60.00	0.1	(2694,8459,53311)
iaal01j2q	09-06-25	08:36:19	60.00	0.5	(2695,8459,53311)
iaal01j4q	09-06-25	08:51:56	60.00	0.6	(2861,8459,53311)
iaal01j5q	09-06-25	08:55:08	60.00	0.4	(2861,8459,53311)
iaal01j7q	09-06-25	09:10:45	60.00	0.7	(2524,8459,53311)
iaal01j8q	09-06-25	09:13:57	60.00	0.9	(2525,8459,53311)

11424\visit2

rootname	obs_date	obs_time	exptime	brth	corrector_pos
iaala2011	09-06-27	16:25:56	120.00	-0.2	(2483,8155,52399)
iaala2021	09-06-27	16:44:45	120.00	0.2	(2141,8155,52399)
iaala2031	09-06-27	17:03:34	120.00	0.5	(2307,8155,52399)
iaala2041	09-06-27	18:00:03	120.00	-0.5	(2645,8155,52399)
iaala2051	09-06-27	18:18:52	120.00	-0.2	(2806,8155,52399)
iaala2061	09-06-27	18:37:41	120.00	0.1	(2478,8155,52399)

11424\visit3

rootname	obs_date	obs_time	exptime	brth	corrector_pos
iaala3011	09-06-29	17:54:38	120.00	-2.4	(2323,7942,52024)
iaala3021	09-06-29	18:13:27	120.00	-2.2	(1994,7942,52024)
iaala3031	09-06-29	18:32:16	120.00	-2.0	(2152,7942,52024)
iaala3041	09-06-29	19:28:37	120.00	-3.2	(2492,7942,52024)
iaala3051	09-06-29	19:47:26	120.00	-3.1	(2660,7942,52024)
iaala3061	09-06-29	20:06:15	120.00	-2.6	(2322,7942,52024)

11434\visit2

rootname	obs_date	obs_time	exptime	brth	corrector_pos
iaata2011	09-07-04	15:59:07	100.00	-2.3	(2318,8047,52277)
iaata2021	09-07-04	16:17:36	200.00	-3.0	(2318,7892,52088)
iaata2031	09-07-04	16:37:45	200.00	-2.5	(2318,7892,52276)
iaata2041	09-07-04	17:30:52	200.00	-1.8	(2318,7892,52461)
iaata2051	09-07-04	17:51:01	200.00	-3.7	(2318,8043,52088)
iaata2061	09-07-04	18:11:10	200.00	-3.1	(2318,8043,52276)
iaata2071	09-07-04	19:06:39	200.00	-1.7	(2318,8043,52461)
iaata2081	09-07-04	19:26:48	200.00	-3.4	(2318,8204,52089)
iaata2091	09-07-04	19:46:57	200.00	-3.1	(2318,8204,52276)
iaata20a1	09-07-04	20:42:25	200.00	-1.7	(2318,8204,52461)
iaata20b1	09-07-04	21:02:34	200.00	-3.6	(2318,8048,52277)

11434\visit51

rootname	obs_date	obs_time	exptime	brth	corrector_pos
iaat51cmq	09-07-06	08:00:35	50.00	-2.0	(2318,8045,52276)
iaat51cnq	09-07-06	08:03:37	50.00	-2.2	(2318,8045,52276)
iaat51cpq	09-07-06	08:19:04	100.00	-2.9	(1988,8045,52276)
iaat51cqq	09-07-06	08:22:56	100.00	-3.0	(1989,8045,52276)
iaat51csq	09-07-06	08:39:13	100.00	-1.1	(2069,8045,52276)
iaat51ctq	09-07-06	08:43:05	100.00	-0.5	(2070,8045,52276)
iaat51cvq	09-07-06	09:25:47	100.00	-0.1	(2147,8045,52276)
iaat51cwq	09-07-06	09:29:39	100.00	-0.7	(2147,8045,52276)
iaat51cyq	09-07-06	09:45:56	100.00	-2.3	(2231,8045,52276)
iaat51czq	09-07-06	09:49:48	100.00	-2.5	(2232,8045,52276)
iaat51d1q	09-07-06	10:06:05	100.00	-2.0	(2314,8045,52276)
iaat51d2q	09-07-06	10:09:57	100.00	-1.7	(2315,8045,52276)
iaat51d4q	09-07-06	11:01:34	100.00	0.1	(2396,8045,52276)
iaat51d5q	09-07-06	11:05:26	100.00	-0.3	(2396,8045,52276)
iaat51d7q	09-07-06	11:21:43	100.00	-2.0	(2485,8045,52276)
iaat51d8q	09-07-06	11:25:35	100.00	-2.1	(2485,8045,52276)
iaat51daq	09-07-06	11:41:52	100.00	-1.6	(2564,8045,52276)
iaat51dbq	09-07-06	11:45:44	100.00	-1.2	(2564,8045,52276)
iaat51ddq	09-07-06	12:37:20	100.00	0.2	(2653,8045,52276)
iaat51deq	09-07-06	12:41:12	100.00	-0.2	(2653,8045,52276)
iaat51dgq	09-07-06	12:57:29	100.00	-1.8	(2316,8045,52276)
iaat51dhq	09-07-06	13:01:21	100.00	-1.8	(2316,8045,52276)

11434\visit52

rootname	obs_date	obs_time	exptime	brth	corrector_pos
iaatb2011	09-07-08	09:29:22	100.00	-0.9	(2437,8045,52087)
iaatb2021	09-07-08	09:47:51	200.00	-2.0	(2436,7891,51902)
iaatb2031	09-07-08	10:08:00	200.00	-0.7	(2437,7891,52086)
iaatb2041	09-07-08	10:54:57	200.00	0.3	(2437,7891,52275)
iaatb2051	09-07-08	11:15:06	200.00	-2.2	(2437,8043,51904)
iaatb2061	09-07-08	11:35:15	200.00	-1.9	(2437,8043,52086)
iaatb2071	09-07-08	12:30:44	200.00	-0.1	(2437,8043,52275)
iaatb2081	09-07-08	12:50:53	200.00	-2.3	(2436,8204,51903)
iaatb2091	09-07-08	13:11:02	200.00	-1.8	(2436,8204,52086)
iaatb20a1	09-07-08	14:06:31	200.00	0.2	(2437,8204,52275)
iaatb20b1	09-07-08	14:26:40	200.00	-2.4	(2437,8047,52088)